

## Ab Initio Study of Hydrogen Adsorption in MOF-5

Kaido Sillar,<sup>†</sup> Alexander Hofmann,<sup>†</sup> and Joachim Sauer<sup>\*,†,‡</sup>

*Institut für Chemie, Humboldt-Universität zu Berlin, Berlin, Germany, and Cluster of Excellence, UNICAT, Berlin*

Received December 23, 2008; E-mail: sek.qc@chemie.hu-berlin.de

**Abstract:** Metal-organic frameworks (MOFs) are promising adsorbents for hydrogen storage. Density functional theory and second-order Møller–Plesset perturbation theory (MP2) are used to calculate the interaction energies between H<sub>2</sub> and individual structural elements of the MOF-5 framework. The strongest interaction,  $\Delta H_{77} = -7.1$  kJ/mol, is found for the  $\alpha$ -site of the OZn<sub>4</sub>(O<sub>2</sub>Ph)<sub>6</sub> nodes. We show that dispersion interactions and zero-point vibrational energies must be taken into account. Comparison of calculations done under periodic boundary conditions for the complete structure with those done for finite models cut from the MOF-5 framework shows that the interactions with H<sub>2</sub> originate mainly from the local environment around the adsorption site. When used within a Multi-Langmuir model, the MP2 results reproduce measured adsorption isotherms (the predicted amount is 6 wt % at 77 K and 40 bar) if we assume that the H<sub>2</sub> molecules preserve their rotational degrees of freedom in the adsorbed state. This allows to discriminate between different isotherms measured for different MOF-5 samples and to reliably predict isotherms for new MOF structures.

### Introduction

The world's increasing demand of energy, depletion of fossil fuels, and environmental concerns necessitate the quest for alternative solutions in current energy production, transfer, and utilization. The change to pollutant-free and more efficient energy exploitation can be achieved with the use of hydrogen as an intermediate medium for storing and transporting energy that is produced from any (preferably renewable) primary source. To meet customer requirements in road transport, the U.S. Department of Energy (DOE) has specified that the on-board hydrogen storage system should store 6 and 9 wt % of hydrogen by the year 2010 and 2015, respectively. Among many materials considered for hydrogen storage, metal-organic frameworks (MOFs) show great potential to fulfill those requirements: an exceptionally high hydrogen uptake of MOF-5 up to 7.1 wt % at approximately 40 bar and 77 K has been determined.<sup>1</sup> Moreover, a neutron powder diffraction study<sup>2</sup> has shown that the MOF-5 host lattice has enough space to hold hydrogen molecules up to 11 wt % at 3.5 K (a pressure of 170 bar is required to reach this loading at 77 K).<sup>1</sup> At room temperature, the maximum hydrogen storage capacity is much lower, in the case of MOF-5 between 0.2 and 0.45 wt %.<sup>3–6</sup> The low hydrogen adsorption at room temperature is attributable to the weak interaction between MOF-5 and hydrogen; the measured hydrogen adsorption enthalpies are ranging from  $-3.5$  to  $-5.2$

kJ/mol.<sup>7–9</sup> To design MOF-based materials with high hydrogen storage capacities at room temperature (with adsorption enthalpies between  $-15$  and  $-40$  kJ/mol)<sup>10–12</sup> detailed understanding of the interactions between MOFs and hydrogen molecules at molecular level is needed.

On the basis of accurate calculations of adsorption energies, molecular statistics, and a Multi-Langmuir adsorption model we will show that reliable ab initio predictions of adsorption isotherms are possible. Even for well-known systems like H<sub>2</sub>/MOF-5 such predictions can help to discriminate between different measurements that yield varying adsorption isotherms.<sup>1,4,5,13–16</sup>

Hydrogen adsorption in MOFs has been studied before with different computational methods.<sup>7,17–24</sup> Density functional theory (DFT) can treat periodic MOF structures and, hence,

<sup>†</sup> Humboldt-Universität zu Berlin.

<sup>‡</sup> Cluster of Excellence, UNICAT, Berlin.

- (1) Kaye, S. S.; Dailly, A.; Yaghi, O. M.; Long, J. R. *J. Am. Chem. Soc.* **2007**, *129*, 14176–14177.
- (2) Yildirim, T.; Hartman, M. R. *Phys. Rev. Lett.* **2005**, *95*, 215504–1215504–4.
- (3) Dailly, A.; Vajo, J. J.; Ahn, C. C. *J. Phys. Chem. B* **2006**, *110*, 1099.
- (4) Panella, B.; Hirscher, M. *Adv. Mater.* **2005**, *17*, 538–541.
- (5) Panella, B.; Hirscher, M.; Pütter, H.; Müller, U. *Adv. Funct. Mater.* **2006**, *16*, 520–524.
- (6) Li, Y.; T.Yang, R. *J. Am. Chem. Soc.* **2006**, *128*, 8136–8137.

- (7) Bordiga, S.; Vitillo, J. G.; Ricchiardi, G.; Regli, L.; Cocina, D.; Zecchina, A.; Arstad, B.; Bjørgen, M.; Hafizovic, J.; Lillerud, K. P. *J. Phys. Chem. B* **2005**, *109*, 18237–18242.
- (8) Kaye, S. S.; Long, J. R. *J. Am. Chem. Soc.* **2005**, *127*, 6506–6507.
- (9) Rowsell, J. L. C.; Yaghi, O. M. *J. Am. Chem. Soc.* **2006**, *128*, 1304–1315.
- (10) Bhatia, S. K.; Myers, A. L. *Langmuir* **2006**, *22*, 1688–1700.
- (11) van den Berg, A. W. C.; Otero Arean, C. *Chem. Commun.* **2008**, 668–681.
- (12) Lochan, R. C.; Head-Gordon, M. *Phys. Chem. Chem. Phys.* **2006**, *8*, 1357–1370.
- (13) Rosi, N. L.; Eckert, J.; Eddaoudi, M.; Vodak, D. T.; Kim, J.; O'Keeffe, M.; Yaghi, O. M. *Science* **2003**, *300*, 1127–1129.
- (14) Wong-Foy, A. G.; Matzger, A. J.; Yaghi, O. M. *J. Am. Chem. Soc.* **2006**, *128*, 3494–3495.
- (15) Rowsell, J. L. C.; Millward, A. R.; Park, K. S.; Yaghi, O. M. *J. Am. Chem. Soc.* **2004**, *126*, 5666–5667.
- (16) Poirier, E.; Dailly, A. *J. Phys. Chem. C* **2008**, *112*, 13047–13052.
- (17) Mulder, F. M.; Dingemans, T. J.; Wagemaker, M.; Kearley, G. *J. Chem. Phys.* **2005**, *317*, 113–118.
- (18) Mueller, T.; Ceder, G. *J. Phys. Chem. B* **2005**, *109*, 17974–17983.
- (19) Samanta, A.; Furuta, T.; Li, J. *J. Chem. Phys.* **2006**, *125*, 084714.
- (20) Garberoglio, G.; Skouliadas, A. I.; Johnson, J. K. *J. Phys. Chem. B* **2005**, *109*, 13094–13103.

include long-range Coulombic interactions, but most of the currently available functionals do not properly take dispersion forces into account. The latter can be included by adding a semiempirical  $1/r^6$  term to DFT energies (DFT+D)<sup>25,26</sup> or by using post Hartree–Fock methods that describe electron correlation explicitly. Because the use of even the simplest of the latter, second-order Møller–Plesset perturbation theory (MP2), is far beyond present computational resources for periodic structures with large unit cells,<sup>28</sup> such calculations are performed only on finite-sized models that represent individual structural elements of the whole MOF framework. So far, relatively small models have been used,<sup>7,21,22,24,29,30</sup> and thus, the effect of increasing model size on the adsorption energies is not known. Also, when even large, localized basis sets with, e.g., diffuse functions are applied, superposition errors (BSSE) are unavoidable, and counterpoise (CP) corrections<sup>31</sup> must be evaluated, preferably with extrapolation to the complete basis set (CBS) limit. Usually this is not done, and this is the reason why calculated hydrogen adsorption energies, which are of the order of 6 kJ/mol, vary over more than 3 kJ/mol.<sup>7,22</sup> Apparent agreement of such results with measured adsorption enthalpies is also questionable because the calculations report energies, whereas experimental results are enthalpies that include zero-point vibrational energy changes and thermal corrections. Furthermore, experiments yield average values because different sites with different adsorption enthalpies are partially populated at a given loading.

The latter effect can be modeled with Monte Carlo or molecular dynamics methods,<sup>20,23,32</sup> but this requires millions of energy calculations which is only possible if parametrized potentials (force fields) are used. The need for parametrization limits the predictive value of this approach and may lead to deviations of the calculated isotherms from observed ones.<sup>32</sup>

Our approach relies on a Multi-Langmuir model which combines adsorption isotherms for individual adsorption sites into an overall isotherm. The free energies for the individual sites are calculated within the rigid rotor, harmonic oscillator, and ideal gas approximation. This makes it possible to determine the contribution of each specific site to the H<sub>2</sub> adsorption capacity of MOF-5 at different temperatures and pressures. The Multi-Langmuir model is applicable because the interactions between H<sub>2</sub> molecules in different adsorption sites and between an H<sub>2</sub> molecule in one of these sites and in a possible “second layer” are much weaker (below 0.5 kJ/mol) than the binding of H<sub>2</sub> in the adsorption sites considered (between 5 and 8 kJ/mol). Another condition is that framework structure and adsorption

volume do not change with the loading, a phenomenon that is observed in cases like MIL-53(Cr) which require different simulation techniques.<sup>33</sup>

For the adsorption energies of the individual sites a hybrid MP2(finite model):DFT(periodic structure) approach is available<sup>34,35</sup> that describes the full crystal lattice with DFT applying periodic boundary conditions and the adsorption site with accurate electron correlation methods. For adsorption and reactions in microporous zeolites where dispersion forces play also an important role this hybrid MP2:DFT scheme yielded significantly more reliable results than periodic DFT or electron correlation calculations on finite-sized models alone.<sup>35,36</sup>

In this study we use DFT on periodic structures and MP2 on finite models to calculate the interaction energy between hydrogen and the different adsorption sites in MOF-5 (comparison is also made with the DFT+D approach). The chosen models turn out large enough that the contributions from the periodic lattice to the interaction energies can be neglected. We also conclude that reliable energies for the individual sites can be obtained from counterpoise corrected MP2/aug-cc-pVTZ results.

## Models

MOF-5 is also known as IRMOF-1 because it is the first member of a series of isorecticular (cubic) metal–organic frameworks (IRMOF)<sup>37–39</sup> with oxide-centered Zn<sub>4</sub>O tetrahedra as nodes linked by organic molecules. In MOF-5 (Figure 1) the organic linker is 1,4-benzenedicarboxylate (BDC). Note that, depending on the synthesis process, residual ZnO species in the pores and lattice interpenetration accompanied by a change of crystal symmetry from cubic to trigonal may have changed the adsorption properties.<sup>40</sup>

Here, we refer to the high crystalline phase with a high specific surface area. Its primitive cell includes two nodes and six linker molecules, corresponding to two OZn<sub>4</sub>(BDC)<sub>3</sub> formula units. The conventional cell (*Fm* $\bar{3}$ *m* symmetry) is cubic and includes eight formula units. Figure 1 shows the location of the studied adsorption sites. Previously the  $\alpha$ -site has been referred to as Cup site, the  $\beta$ -site as ZnO<sub>3</sub> site, the  $\gamma$ -site as ZnO<sub>2</sub> site, and the Linker site as Hex site.<sup>2</sup> There are four  $\alpha$ - and four  $\beta$ -sites, twelve  $\gamma$ -sites, and six Linker sites per Zn<sub>4</sub>O(BDC)<sub>3</sub> formula unit, and the full occupation of these sites would represent a full “monolayer” of H<sub>2</sub> molecules adsorbed on the “internal” surface of MOF-5.

In this work, in addition to the periodic structures, finite-sized models cut out from the MOF-5 framework are studied (Figure 2). For the Zn<sub>4</sub>O nodes of the framework two models of different sizes are used. The smaller one consists of an oxide-centered Zn<sub>4</sub>O tetrahedron with six formate anions as ligands

(21) Sagara, T.; Klassen, J.; Ortony, J.; Ganz, E. *J. Chem. Phys.* **2005**, *123*, 014701–1014701–4.

(22) Sagara, T.; Klassen, J.; Ganz, E. *J. Chem. Phys.* **2004**, *121*, 12543–12547.

(23) Yang, Q.; Zhong, C. *J. Phys. Chem. B* **2005**, *109*, 11862–11864.

(24) Hübner, O.; Glöck, A.; Fichtner, M.; Kloppe, W. *J. Phys. Chem. A* **2004**, *108*, 3019–3023.

(25) Grimme, S. *J. Comput. Chem.* **2004**, *25*, 1463–1473.

(26) Grimme, S. *J. Comput. Chem.* **2006**, *27*, 1787–1799.

(27) Pisani, C.; Busso, M.; Capecchi, G.; Casassa, S.; Dovesi, R.; Maschio, L.; Zicovich-Wilson, C.; Schütz, M. *J. Chem. Phys.* **2005**, *112*, 094113.

(28) Pisani, C.; Maschio, L.; Casassa, S.; Halo, M.; Schütz, M.; Usvyat, D. *J. Comput. Chem.* **2008**, *29*, 2113–2124.

(29) Klontzas, E.; Mavrandonakis, A.; Froudakis, G. E.; Carissan, Y.; Kloppe, W. *J. Phys. Chem. C* **2007**, *111*, 13635–13640.

(30) Kuc, A.; Heine, T.; Seifert, G.; Duarte, H. A. *Chem. Eur. J.* **2008**, *14*, 6597–6600.

(31) Boys, S. F.; Bernardi, F. B. *Mol. Phys.* **1970**, *19*, 553–566.

(32) Frost, H.; Düren, T.; Snurr, R. Q. *J. Phys. Chem. B* **2006**, *110*, 9565–9570.

(33) Salles, F.; Ghoufi, A.; Maurin, G.; Bell, R. G.; Mellot-Draznieks, C.; Ferey, G. *Angew. Chem., Int. Ed.* **2008**, *47*, 8487–8491.

(34) Tuma, C.; Sauer, J. *Chem. Phys. Lett.* **2004**, *387*, 388–394.

(35) Tuma, C.; Sauer, J. *Phys. Chem. Chem. Phys.* **2006**, *8*, 3955–3965.

(36) Svelle, S.; Tuma, C.; Rozanska, X.; Kerber, T.; Sauer, J. *J. Am. Chem. Soc.* **2009**, *131*, 816–825.

(37) Li, H.; Eddaoudi, M.; Groy, T. L.; Yaghi, O. M. *J. Am. Chem. Soc.* **1998**, *120*, 8571–8572.

(38) Li, H.; Eddaoudi, M.; O’Keeffe, M.; Yaghi, O. M. *Nature* **1999**, *402*, 276–279.

(39) Eddaoudi, M.; Kim, J.; Rosi, N.; Vodak, D.; Wachter, J.; O’Keeffe, M.; Yaghi, O. M. *Science* **2002**, *295*, 469–472.

(40) Hafizovic, J.; Bjorgen, M.; Olsbye, U.; Dietzel, P. D. C.; Bordiga, S.; Prestipio, C.; Lamberti, C.; Lillerud, K.-P. *J. Am. Chem. Soc.* **2007**, *129*, 3612–3620.

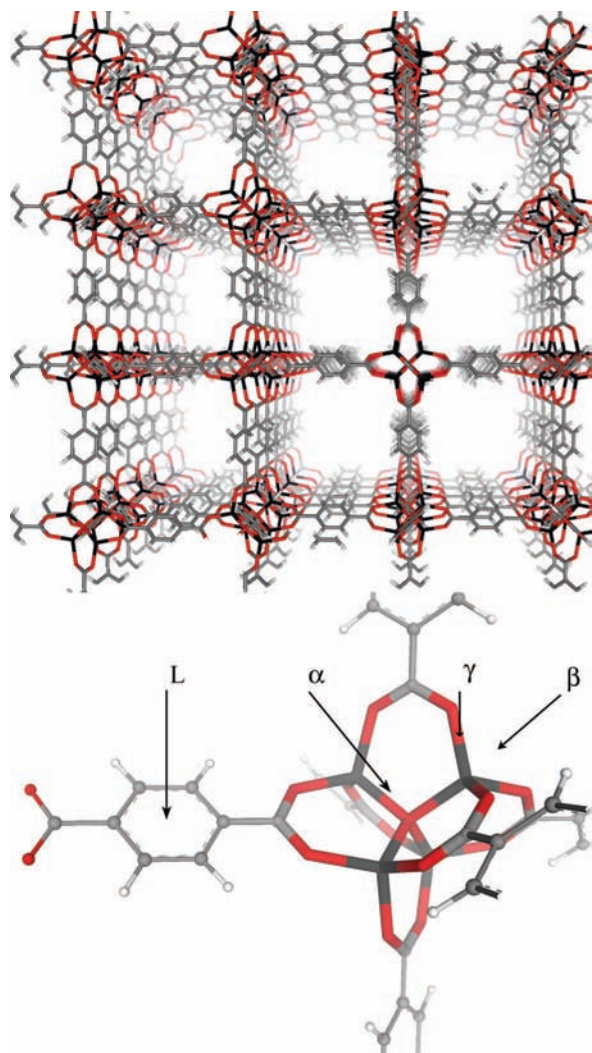


**Figure 1.** The crystal structure of MOF-5 and the locations of the adsorption sites studied in the MOF-5 framework.

at the edges of the tetrahedron,  $\text{OZn}_4(\text{CO}_2\text{H})_6$ . In the bigger model the six ligands are benzoate instead of formate anions,  $\text{OZn}_4(\text{CO}_2\text{Ph})_6$ . The small and big models will be referred to as formate model and benzoate model, respectively. For the organic part of the framework (linker) a model is used that consists of two formate models connected by a benzene ring.

## Methods

**DFT Calculations.** Were performed with the Perdew–Burke–Ernzerhofer (PBE) exchange–correlation functional employing the VASP<sup>41,42</sup> program package. Valence electrons were described by a plane wave basis set with a kinetic energy cutoff of 400 eV, and the core, by projector augmented waves. The Brillouin zone was sampled with a  $2 \times 2 \times 2$  Monkhorst–Pack k-point mesh.<sup>43</sup> For the PBE calculations with periodic boundary conditions the equilibrium volume of the primitive cell was obtained by fitting a Murnaghan equation of state to a series of fixed-volume relaxed structures. The minimum energy is obtained for a lattice constant of the conventional unit cell  $a_C = 26.131 \text{ \AA}$  ( $Fm\bar{3}m$  symmetry). This is in good agreement with lattice constant determined experimentally<sup>2</sup> ( $a_C = 25.91 \text{ \AA}$ ) and obtained in previous theoretical

studies.<sup>18,44</sup> In all following periodic DFT calculations this cell parameter was kept constant. For DFT calculations on finite models a cubic computational box with length of  $25 \text{ \AA}$  was used to avoid interactions between periodic images.

The PBE+Dispersion calculations under periodic boundary conditions were performed using the QMOT program<sup>45–47</sup> that combines PBE energy and force calculations with the dispersion term (“Grimme-2006” parameters)<sup>26</sup> using an additional interface<sup>48</sup>

**MP2 Calculations.** Were performed with the rice2 module<sup>49–51</sup> of the TURBOMOLE V5.10 program package.<sup>52</sup> Only the valence shell electrons were correlated (frozen core approximation), and the resolution of identity (RI) approximation also known as density fitting was employed.<sup>53</sup> The def2-TZVP basis sets of Ahlrichs et al.<sup>54,55</sup> and the correlation-consistent (aug-)cc-pVXZ (where X = T and Q) basis sets by Dunning et al.<sup>56,57</sup> were applied. For example, the contracted functions for def2-TZVP and aug-cc-pVTZ basis sets on Zn/O,C/H are [6s5p4d1f/5s3p2d1f/3s1p] and [6s6p5d3f2g/5s4p3d2f/4s3p2d], respectively. For Zn the (aug-)cc-pVXZ-PP basis set<sup>58,59</sup> is used with the Stuttgart–Koeln MCDHF RSC ECP.<sup>60</sup> For RI calculations appropriate auxiliary basis functions were applied.<sup>55,61,62</sup> The counterpoise scheme is applied to correct calculated adsorption energies for BSSE.<sup>31</sup> BSSE-corrected MP2 adsorption energies calculated with Dunning’s basis sets for X = T and Q are extrapolated to the CBS limit. CBS(D,T) denotes the extrapolation from aug-cc-pVDZ and aug-cc-pVTZ basis sets. For the Hartree–Fock (HF) contribution to the MP2 adsorption energy an exponential scheme<sup>63,64</sup> is chosen, whereas an inverse power law<sup>65</sup> is applied to the correlation energy contribution.

**Vibrational Frequencies.** Were calculated within the harmonic approximation on fully MP2/def2-TZVP optimized finite-sized models. No scaling was applied. Calculations on formate models show that upon H<sub>2</sub> adsorption on the  $\alpha$ -site the vibrational frequencies of the model change only by 1.2% on average. The largest changes are associated with the four frequencies below  $50 \text{ cm}^{-1}$  among which one frequency is increased from 20 to  $29 \text{ cm}^{-1}$ . This does not change the calculated adsorption enthalpies but decreases the adsorption entropy by 7 J/K. For the H<sub>2</sub> adsorption on  $\beta$ - and  $\gamma$ -sites the largest changes in the

- (44) Civalleri, B.; Napoli, F.; Noel, Y.; Roetti, C.; Dovesi, R. *CrystEng-Comm* **2006**, *8*, 364–371.
- (45) Sierka, M.; Sauer, J. *J. Chem. Phys.* **2000**, *112*, 6983–6996.
- (46) Sierka, M.; Sauer, J. *Faraday Discuss.* **1997**, *106*, 41–62.
- (47) Sauer, J.; Sierka, M. *J. Comput. Chem.* **2000**, *21*, 1470–1493.
- (48) Kerber, T.; Sierka, M.; Sauer, J. *J. Comput. Chem.* **2008**, *29*, 2088–2097.
- (49) Hättig, C.; Weigend, F. *J. Chem. Phys.* **2000**, *113*, 5154–5161.
- (50) Hättig, C. *J. Chem. Phys.* **2003**, *118*, 7751–7761.
- (51) Hättig, C.; Hellweg, A.; Köhn, A. *Phys. Chem. Chem. Phys.* **2006**, *8*, 1159–1169.
- (52) Ahlrichs, R.; Bär, M.; Häser, M.; Horn, H.; Kölmel, C. *Chem. Phys. Lett.* **1989**, *162*, 165–169.
- (53) Dunlap, B. I.; Conolly, J. W. D.; Sabin, J. R. *J. Chem. Phys.* **1979**, *71*, 4993–4999.
- (54) Weigend, F.; Ahlrichs, R. *Phys. Chem. Chem. Phys.* **2005**, *7*, 3297–3305.
- (55) Hellweg, A.; Hättig, C.; Höfener, S.; Klopper, W. *Theor. Chem. Acc.* **2007**, *117*, 587–597.
- (56) Dunning Jr, T. H. *J. Chem. Phys.* **1989**, *90*, 1007–1023.
- (57) Kendall, R. A.; Dunning, T. H., Jr.; Harrison, R. J. *J. Chem. Phys.* **1992**, *96*, 6796–6806.
- (58) Balabanov, N. B.; Peterson, K. A. *J. Chem. Phys.* **2005**, *123*, 064107.
- (59) Peterson, K. A.; Puzzarini, C. *Theor. Chem. Acc.* **2005**, *114*, 283–296.
- (60) Figgen, D.; Rauhut, G.; Dolg, M.; Stoll, H. *Chem. Phys.* **2005**, *311*, 227–244.
- (61) Weigend, F.; Häser, M.; Patzelt, H.; Ahlrichs, R. *Chem. Phys. Lett.* **1998**, *294*, 143.
- (62) Weigend, F.; Köhn, A.; Hättig, C. *J. Chem. Phys.* **2002**, *116*, 3175.
- (63) Halkier, A.; Helgaker, T.; Jørgensen, P.; Klopper, W.; Olsen, J. *Chem. Phys. Lett.* **1999**, *302*, 437–466.
- (64) Jensen, F. *Theor. Chem. Acc.* **2005**, *113*, 267–273.

(41) Kresse, G.; Furthmüller, J. *Comput. Mater. Sci.* **1996**, *6*, 15–50.  
 (42) Kresse, G.; Furthmüller, J. *Phys. Rev. B* **1996**, *54*, 11169–11186.  
 (43) Monkhorst, H. J.; Pack, J. D. *Phys. Rev. B* **1976**, *13*, 5188–5192.



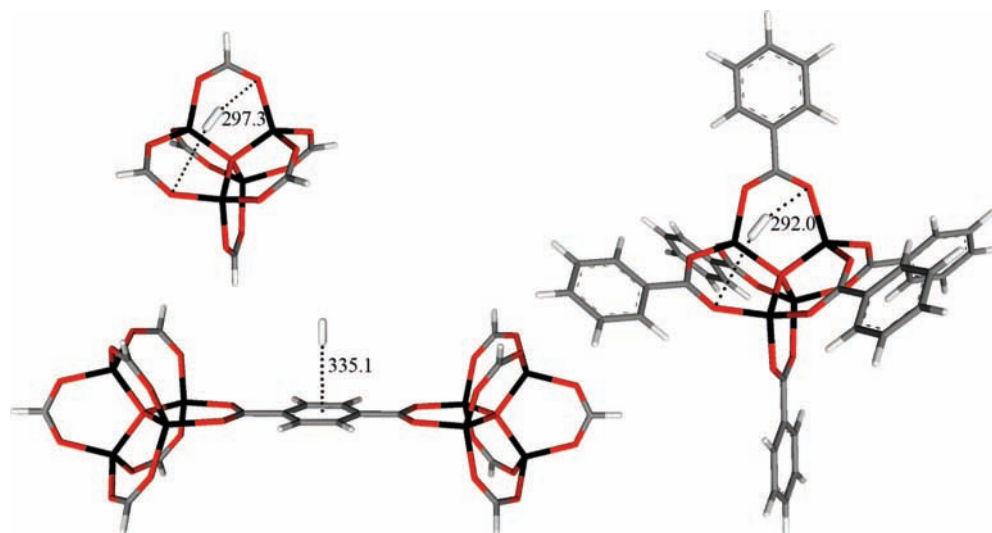


**Figure 2.** “Formate” (top left,  $\text{OZn}_4(\text{CO}_2\text{H})_6$ ), and “benzoate” (right,  $\text{OZn}_4(\text{CO}_2\text{Ph})_6$ ) models for the framework node and “Linker” model (left bottom) for the 1,4-benzenedicarboxylate in MOF-5. All with adsorbed hydrogen molecules. Distances in pm.

vibrational frequencies of the model do not exceed 6.5%. Also, the stretching vibrational frequency of adsorbed  $\text{H}_2$  is the same when calculated with the full Hessian or using a partial Hessian considering only the 6 degrees of freedom of the adsorbed  $\text{H}_2$  molecule. Thus, zero-point vibrational energies and thermal corrections for the adsorption enthalpies as well as free energies were obtained from partial Hessians calculated for the benzoate models.

**Adsorption Isotherms.** Were calculated according to the multisite Langmuir equation<sup>66</sup> which yields the total surface coverage,  $\theta$ , as the sum of  $\text{H}_2$  adsorbed on different sites.

$$\theta = x_\alpha \frac{K_\alpha P}{1 + K_\alpha P} + x_\beta \frac{K_\beta P}{1 + K_\beta P} + x_\gamma \frac{K_\gamma P}{1 + K_\gamma P} + x_\gamma \frac{K_\alpha K_\gamma P^2}{1 + K_\alpha P + K_\alpha K_\gamma P^2} \quad (1)$$

The last term in this equation gives the adsorption on  $\gamma$ -sites and takes into account that  $\text{H}_2$  can bind to  $\gamma$ -sites only if  $\text{H}_2$  is already adsorbed on  $\alpha$ -site first. The fraction of sites  $x_{\text{site}} = N_{\text{site}}/N$  is the ratio of the number  $N_{\text{site}}$  of specific adsorption sites per  $\text{Zn}_4\text{O}(\text{BDC})_3$  formula unit and the total number of sites per formula unit,  $N = 26$ .

$K$  is adsorption equilibrium constant

$$K = \frac{Q_{\text{surf}}^{\text{H}_2}}{Q_{\text{gas}}^{\text{H}_2}} e^{-\frac{D_0}{RT}} \quad (2)$$

where  $Q_{\text{surf}}^{\text{H}_2}$  and  $Q_{\text{gas}}^{\text{H}_2}$  are the partition functions of hydrogen on the surface and in gas phase, respectively, and  $D_0$  is interaction energy between hydrogen and the MOF surface at 0 K, i.e. including the zero-point energy changes,  $\Delta\text{ZPE}$ ,

$$D_0 = \Delta E + \Delta\text{ZPE} \quad (3)$$

where  $\Delta E$  is the CP-corrected MP2/CBS(D,T) adsorption energy calculated on MP2/def2-TZVP optimized benzoate models.

**Table 1.** Dependence of the  $\text{H}_2$  Adsorption Energy (kJ/mol) on the Basis Set for the Formate Model

	MP2	CP-corrected MP2	MP2 with diffuse functions	CP-corrected MP2 with diffuse functions
def2-TZVP	-5.2	-2.7	–	–
cc-pVTZ	-7.1	-3.2	-8.3	-5.4 <sup>a</sup>
CBS(D,T)				-6.1
cc-pVQZ	-6.5	-4.9	-7.5 <sup>b</sup>	-5.8 <sup>b</sup>
CBS limit	-7.0	-5.8	-6.7	-6.0

<sup>a</sup> Calculations at the MP2/def2-TZVP reference structure also yield -5.4 kJ/mol. <sup>b</sup> On the cc-pVQZ optimized structure.

The rotational partition function,  $q_{\text{rot}}$ , is computed by direct summation of the first 50 rotational levels,<sup>67</sup>

$$q_{\text{rot}} = \frac{1}{4} \sum_{J \text{ even}} (2J + 1) e^{-\Theta_{\text{rot}} J(J+1)/T} + \frac{3}{4} \sum_{J \text{ odd}} (2J + 1) e^{-\Theta_{\text{rot}} J(J+1)/T} \quad (4)$$

where  $J$  is the rotational quantum number and  $\Theta_{\text{rot}}$  is the rotational temperature.

## Results and Discussion

**Comparison of Different Methods for Adsorption Energies and Structures.** Previous studies have shown that MP2 adsorption energies are very dependent on the basis set applied and on the BSSE. For example, for hydrogen binding to the formate model, BSSE corrected adsorption energies range from -3.1 to -5.1 kJ/mol,<sup>7,29,30</sup> whereas uncorrected adsorption energies can be as large as -6.9 kJ/mol.<sup>22</sup> Table 1 shows the MP2 results of this study with increasing basis set size. Without diffuse functions the BSSE can reach 50%. Addition of diffuse functions (aug-cc-pVXZ) reduces the basis set dependence significantly and yields a complete basis set (CBS) limit of -6.0 kJ/mol. The MP2/aug-cc-pVTZ result (-5.4 kJ/mol) is only 0.6 kJ/mol smaller than this limit.

Because calculations with quadruple- $\zeta$  basis set are not feasible on benzoate models, we use in the following adsorption

(65) Helgaker, T.; Klopper, W.; Koch, H.; Noga, J. *J. Chem. Phys.* **1997**, *106*, 9639–1997.

(66) Dill, K. A.; Bromberg, S. *Molecular Driving Forces: Statistical Thermodynamics in Chemistry and Biology*; Garland Science: New York, 2003.

(67) McQuarrie, D. A. *Statistical Mechanics*; University Science Books: Mill Valley, CA, 2000.

**Table 2.** Hydrogen Adsorption Energies (kJ/mol) Calculated with Different Methods on Periodic PBE Structures where Hydrogen Molecules Occupy Only  $\alpha$ - or  $\beta$ -Sites of One Node of the Framework and on Formate and Benzoate Model Models Cut Out from these Periodic PBE Structures; MP2 Energies are Corrected for BSSE

		formate model	benzoate model	periodic	
$\alpha$ -site	PBE/planewaves	-1.6	-1.8	-1.8	
	PBE+Disp	-5.3	-6.3	-6.3 (-9.6) <sup>a</sup>	
	MP2/aug-cc-pVTZ	-4.1	-5.9	-	
	HF/CBS(D,T)	1.1	0.9	-	
	MP2/CBS(D,T)	-4.4	-6.0	-	
	hybrid MP2/aug-cc-pVTZ:PBE+Disp	-5.1	-5.9	-	
	hybrid MP2/CBS(D,T):PBE+Disp	-5.4	-6.0	-	
	$\beta$ -site	PBE/planewaves	-1.1	-2.1	-2.1
		PBE+Disp	-2.6	-4.7	-4.9 (-5.7) <sup>a</sup>
MP2/aug-cc-pVTZ		-1.7	-3.8	-	
HF/CBS(D,T)		0.5	0.0	-	
MP2/CBS(D,T)		-1.7	-3.9	-	
hybrid MP2/aug-cc-pVTZ:PBE+Disp		-4.0	-4.0	-	
hybrid MP2/CBS(D,T):PBE+Disp		-4.0	-4.1	-	

<sup>a</sup> Adsorption energy for optimized PBE+Disp structure.

energies that are extrapolated to the CBS limit from BSSE-corrected MP2 adsorption energies calculated with aug-cc-pVDZ and aug-cc-pVTZ basis sets on MP2/def2-TZVP optimized structures. For the formate model, this CBS(D,T) adsorption energy (-6.1 kJ/mol) is very close to the value obtained from the extrapolation using the aug-cc-pVTZ and aug-cc-pVQZ basis sets on the MP2/aug-cc-pVTZ structure (-6.0 kJ/mol). The estimates for the remaining uncertainties concerning neglect of higher-order electron correlation effects show slight increase in the H<sub>2</sub> binding energy for the  $\alpha$ -site (about 0.4 kJ/mol, see Supporting Information) which may be partially compensated by a small decrease of 0.1 kJ/mol due to larger basis sets (Table 1). For the Linker site the inclusion of higher excitations and the use of larger basis sets is expected<sup>21,24</sup> to decrease the MP2 binding energy by about 0.75 kJ/mol. In total, these effects would change the amount of adsorbed H<sub>2</sub> from 6.0 to 5.6 wt % at 77 K and 40 bar, respectively, indicating that the obtained adsorption energies and isotherms are likely to be very close to the converged results.

To investigate the effect of the model size on the hydrogen adsorption energies first DFT calculations were performed for a periodic structure in which hydrogen molecules occupy either all four  $\alpha$ -sites or all four  $\beta$ -sites belonging to one of the two OZn<sub>4</sub> nodes in the primitive cell (Table 2). This corresponds to loading of four H<sub>2</sub> molecules per OZn<sub>4</sub>(BDC)<sub>3</sub> formula unit. For the DFT structure single-point calculations are made on the formate and benzoate models, and the results are reported in Table 2. The PBE and PBE+Dispersion results show that the adsorption energies are converged to the periodic value already for the benzoate model.

Comparison of DFT with DFT+Dispersion and of MP2 with Hartree-Fock (HF) indicates that dispersion is the major contribution to H<sub>2</sub> binding. Note, however, that PBE may effectively already include some dispersion in the region of overlapping densities<sup>68</sup> and that the correlation part of the interaction energy,  $\Delta E_{\text{cor}} = \Delta E(\text{MP2}) - \Delta E(\text{HF})$ , is dominated by dispersion, but also includes additional effects.<sup>69</sup> Consistent

**Table 3.** On Benzoate Models at MP2/def2-TZVP Calculated H<sub>2</sub> Bond Lengths,  $d(\text{H-H})$ , Distances between Hydrogen Atom in Adsorbed H<sub>2</sub> and the Closest Atoms in MOF-5 Framework,  $d(\text{H}_2 \cdots \text{MOF})$ , Shifts in H<sub>2</sub> Vibrational Frequencies (Relative to Hydrogen in Gas Phase,  $\Delta\omega$ ) Upon Adsorption,  $\Delta\omega(\text{H-H})$ , and Vibrational Frequencies of Hydrogen Molecules Relative to the Surface of the MOF,  $\omega(\text{H}_2 \cdots \text{MOF})$

site	$d(\text{H-H})$ pm	$d(\text{H}_2 \cdots \text{MOF})$ pm	$\Delta\omega(\text{H-H})^d$ cm <sup>-1</sup>	$\omega(\text{H}_2 \cdots \text{MOF})$ cm <sup>-1</sup>
$\alpha$	74.08	292.0 <sup>a</sup>	-50.4	104.7, 119.2, 157.9, 180.9 <sup>e</sup> , 253.6 <sup>e</sup>
	73.94	298.8 <sup>a</sup>	-30.2	47.9, 78.0, 90.4, 163.0 <sup>e</sup> , 186.4 <sup>e</sup>
$\beta$	73.91	296.9 <sup>a,b</sup>	-26.0	49.1, 93.1, 110.9, 114.0 <sup>e</sup> , 225.2 <sup>e</sup>
L	73.93	335.1 <sup>c</sup>	-29.6	68.5, 75.2, 101.1 <sup>e</sup> , 126.7 <sup>e</sup> , 157.1

<sup>a</sup> Distance to the closest oxygen atoms in MOF-5 framework.

<sup>b</sup> Distance to the closest hydrogen atoms in benzene rings is 290.5 pm.

<sup>c</sup> Distance to the center of benzene ring. <sup>d</sup> Free H<sub>2</sub>: 4544.7 cm<sup>-1</sup>.

<sup>e</sup> Vibrations that are substituted with rotations.

with these findings, for the formate and benzoate models of the  $\alpha$ -site,  $\Delta E_{\text{cor}}$  (-5.5 and -6.9, respectively) is larger than the dispersion correction to PBE (-3.7 and -4.5 kJ/mol, respectively). The increase of these energies with increasing the model from formate to benzoate shows that dispersion interactions with the benzene rings makes a significant contribution to the total H<sub>2</sub> binding energies. For the formate and benzoate models of the  $\beta$ -site,  $\Delta E_{\text{cor}}$  (-2.2 and -3.9 kJ/mol, respectively) and the dispersion correction to PBE (-1.5 and -2.6 kJ/mol, respectively) show the same trend, but are smaller. Since these interactions are missing in all DFT calculations even on periodic structures, this results in wrong relative stabilities of hydrogen adsorbed on different sites. According to periodic DFT H<sub>2</sub> is more strongly (by 0.3 kJ/mol) bound to  $\beta$ -sites than to  $\alpha$ -sites, whereas periodic DFT+Dispersion and MP2 calculations show the opposite trend, binding on  $\alpha$ -sites is 1.4 and 2.1 kJ/mol stronger, respectively. Agreement between DFT+Dispersion results for the benzoate model and the periodic structure shows that it is mainly the local environment around the adsorption site that determines the adsorption properties of MOF-5 and modeling of hydrogen adsorption with relatively large, but finite models (Figure 2) is well justified.

From the results presented so far we conclude that MP2 calculations should be performed for the benzoate model of the nodes and the linker model and that the aug-cc-pVTZ basis set should be used with CP corrections for the energies. A further question is which reference structure should be used. Structure optimizations at this level, as reported in Table 1 for the formate model, would be extremely costly for the benzoate models, but can be avoided. It turns out that the CP-MP2/aug-cc-pVTZ H<sub>2</sub> adsorption energies ( $\alpha$ -site) for the formate model calculated at the MP2/def2-TZVP and MP2/aug-cc-pVTZ structures (cf. Table 1) are the same, both are -5.4 kJ/mol. For the benzoate model, the CP-corrected MP2/aug-cc-pVTZ//MP2/def2-TZVP adsorption energy is -7.6 kJ/mol.

Table 3 presents MP2/def2-TZVP structure data for H<sub>2</sub> adsorption on the different sites for the benzoate models. Because the interactions are stronger, the distances between adsorbed hydrogen and the MOF surface is 5 pm shorter ( $\alpha$ -site) than for the formate model and the H-H bond length of adsorbed hydrogen is 0.1 pm longer. The calculated harmonic frequencies of H<sub>2</sub> adsorbed on formate and benzoate models are 4511 and 4494 cm<sup>-1</sup>, respectively. The calculated frequency shift upon adsorption is -50 cm<sup>-1</sup> (Table 3) relative to the harmonic frequency of H<sub>2</sub> in the gas phase (4545 cm<sup>-1</sup>). The

(68) Wesolowski, T. A.; Parisel, O.; Ellinger, Y.; Weber, J. J. *Phys. Chem. A* **1997**, *101*, 7818-7825.

(69) Chalasiński, G.; Szczesniak, M. M. *Mol. Phys.* **1988**, *63*, 205-224.

**Table 4.** Adsorption Energies at 0K,  $\Delta E$ , Change in Zero-Point Vibrational Energies upon Adsorption of H<sub>2</sub>,  $\Delta ZPE$ , and Adsorption Enthalpies, Entropies, and Gibbs Free Energies at 77 K and 1 bar ( $\Delta H_{77}$ ,  $\Delta S_{77}$ ,  $\Delta G_{77}$ ) Calculated on Benzoate Models at MP2/def2-TZVP; All in kJ/mol

site	$\Delta E^a$	adsorbed H <sub>2</sub> has 2 rotational and 3 vibrational degrees of freedom				adsorbed H <sub>2</sub> has 5 vibrational degrees of freedom		
		$\Delta ZPE$	$\Delta H_{77}$	$-\Delta S_{77}$	$\Delta G_{77}$	$\Delta ZPE$	$\Delta H_{77}$	$-\Delta S_{77}$
$\alpha(D_2)$	-8.0 (-7.6)	1.4	-7.4	6.4	-1.0	3.2	-6.0	6.7
$\alpha$	-8.0 (-7.6)	2.0	-7.1	6.2	-0.9	4.6	-5.2	6.3
$\beta$	-4.6 (-4.4)	1.1	-4.1	5.3	1.2	3.2	-2.6	5.3
$\gamma$	-5.2 (-5.0)	1.4	-4.6	5.5	0.9	3.4	-3.1	5.5
L	-5.1 (-4.8)	1.6	-4.3	5.8	1.5	3.0	-3.3	5.4

<sup>a</sup> CP-corrected MP2/CBS(D,T)/MP2/def2-TZVP; CP-corrected MP2/aug-cc-pVTZ//MP2/def2-TZVP in parentheses.

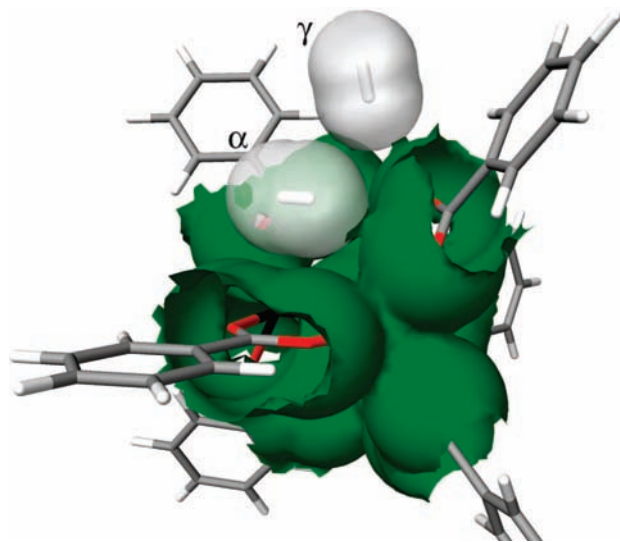


**Figure 3.** Van der Waals surfaces for the benzoate model with adsorbed H<sub>2</sub> molecules in  $\alpha$ - and  $\gamma$ -positions.

IR spectra recorded by Vitillo et al.<sup>7,70</sup> show indeed an absorption maximum at 4112 cm<sup>-1</sup> which corresponds to frequency shift of -49 cm<sup>-1</sup> relative to para-hydrogen in gas phase. Also the heat of adsorption of -7.4 kJ/mol derived from intensity changes with the temperature is in good agreement with the  $\Delta H_{77} = -7.1$  kJ/mol ( $\Delta E = -8.0$  kJ/mol) we calculate for the  $\alpha$ -site (Table 4). A recent diffuse reflectance IR study<sup>71</sup> does not reveal directly vibrational transitions at this energy, but a shift of  $\Delta\omega(H-H) = -49.3$  cm<sup>-1</sup> can be derived from the S(0) rovibrational band at 4448.5 cm<sup>-1</sup>. This confirms that our calculations reproduce well experimentally measured frequency shifts of hydrogen molecule upon adsorption. The calculated frequency shifts of hydrogen adsorbed on all sites studied are also presented in Table 3.

**MP2 Results for Use with Multi-Langmuir Description of Adsorption.** Table 4 shows CP-corrected MP2/CBS(D,T)/MP2/def2-TZVP energies for H<sub>2</sub> adsorption on all sites using the benzoate models. Figure 3 shows the structure of H<sub>2</sub> in a  $\gamma$ -site next to an H<sub>2</sub> in an  $\alpha$ -site. If there were no H<sub>2</sub> molecule in the  $\alpha$ -position, a molecule in the less stable  $\gamma$ -position (-5.2 kJ/mol, Table 4) would move into the more stable  $\alpha$ -position (-8.0 kJ/mol). The H<sub>2</sub>-H<sub>2</sub> pair interaction in the complex is -0.19 kJ/mol (CP-corr. MP2/CBS(D,T)/def2-TZVP), and the distance between the bond midpoints is 355 pm. For two isolated H<sub>2</sub> molecules in the most stable T-shape configuration we get -0.32 kJ/mol at 368 pm, whereas the most accurate ab initio H<sub>2</sub> potential yields -0.48

kJ/mol at 335 pm.<sup>72</sup> Thus, it is the H<sub>2</sub>/MOF5 interaction that determines the position of the H<sub>2</sub> molecules. The very weak H<sub>2</sub>-H<sub>2</sub> interaction compared to the strong H<sub>2</sub>/MOF5 interaction makes the Langmuir model work. Further evidence comes from the following comparison. Table 1 shows MP2/def2-TZVP binding energies for the  $\alpha$ -site (formate model). There are four  $\alpha$ -sites around such a model (which would belong to different MOF cavities). If this calculation is done for one H<sub>2</sub> molecule/three empty sites and for four H<sub>2</sub> molecules/no empty site, the average binding energies per H<sub>2</sub> molecule are -5.18 and -5.15 kJ/mol, respectively.

Upon adsorption the three translational and two rotational degrees of freedom of the H<sub>2</sub> molecule in the gas phase may be converted into five vibrations relative to the adsorption site. The corresponding harmonic frequencies are also presented in Table 3. These vibrations make substantial contributions to the free energy of adsorption as the data in the right part of Table 4 show. Comparison of experimentally measured<sup>1,14-16</sup> and calculated adsorption isotherms in Figure 4 shows that adsorption isotherms derived from free energies for the adsorption sites calculated this way underestimate the amount of adsorbed hydrogen. However, experimental evidence shows that H<sub>2</sub> molecules can retain both of their rotational degrees of freedom when weakly adsorbed in zeolites<sup>73,74</sup> or other microporous frameworks.<sup>70,75</sup> Recently, this was confirmed also for hydrogen adsorbed in MOF-5.<sup>71</sup> If we assume that adsorbed hydrogen molecules have preserved their rotational degrees of freedom and that only translations are converted into vibrations on adsorption (see the data in the left part of Table 4), then the calculated adsorption isotherms are in very good agreement with experimental ones (Figure 4).

The free rotator-like behavior of the hydrogen molecule can be rationalized by the very flat potential energy surface at the adsorption site. For the almost spherical hydrogen molecule with a small moment of inertia (large rotational constant) this means that the orientation-dependent intermolecular interactions are quite small. The highest rotational barriers estimated from two different INS experiments<sup>76,77</sup> are 0.6 and 1.8 kJ/mol.

The data presented in Table 4 make it possible to explain how retaining the rotational freedom of hydrogen molecules in the adsorbed state increases the predicted amount of adsorbed hydrogen. The adsorption enthalpies are larger (absolute terms) when hydrogen on the surface is treated as a free rotator. Of the

(70) Vitillo, J. G.; Regli, L.; Chavan, S.; Ricchiardi, G.; Spoto, G.; Dietzel, P. D. C.; Bordiga, S.; Zecchina, A. *J. Am. Chem. Soc.* **2008**, *130*, 8386-8396.

(71) FitzGerald, S. A.; Allen, K.; Landerman, P.; Hopkins, J.; Matters, J.; Myers, R. *Phys. Rev. B* **2008**, *77*, 224301-1224301-19.

(72) Patkowski, K.; Cencek, W.; Jankowski, P.; Szalewicz, K.; Mehl, J. B.; Garberoglio, G.; Harvey, A. H. *J. Chem. Phys.* **2008**, *129*, 094304-1094304-19.

(73) Kazansky, V. B. *J. Mol. Catal. A* **1999**, *141*, 83-94.

(74) Nicol, J. M.; Eckert, J.; Howard, J. *J. Phys. Chem.* **1988**, *92*, 7117-7121.

(75) Forster, P. M.; Eckert, J.; Heiken, B. D.; Parise, J. B.; Yoon, J. W.; Jhung, S. H.; Chang, J.-S.; Cheetham, A. K. *J. Am. Chem. Soc.* **2006**, *128*, 16846-16850.

(76) Rowsell, J. L. C.; Eckert, J.; Yaghi, O. M. *J. Am. Chem. Soc.* **2005**, *127*, 14904-14910.

(77) Mulder, F. M.; Dingemans, T. J.; Schimmel, H. G.; Ramirez-Cuesta, A. J.; Kearley, G. *J. Chem. Phys.* **2008**, *351*, 72-76.



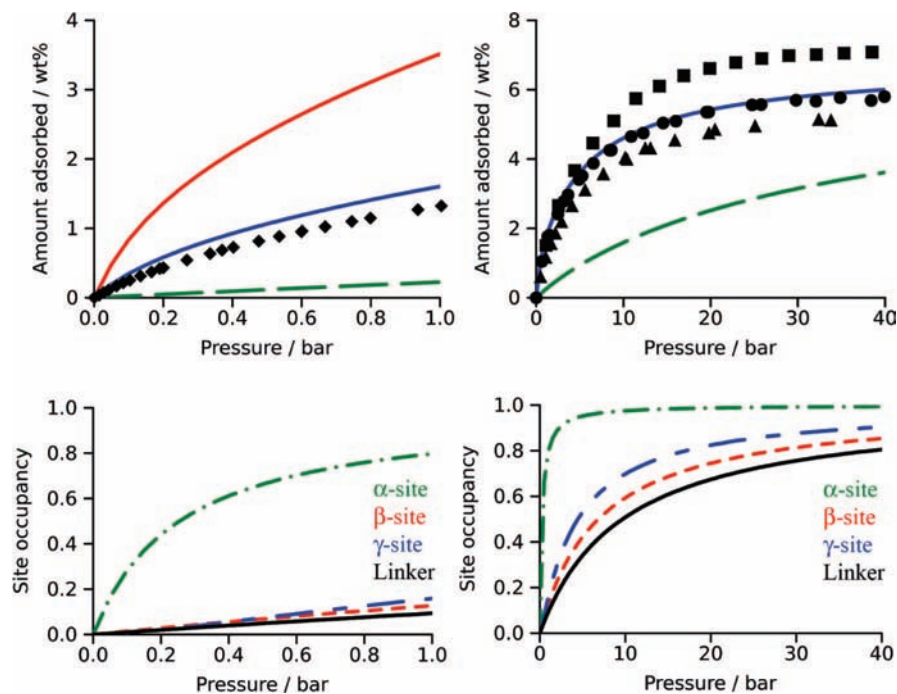


**Figure 4.** (Top) Comparison of calculated H<sub>2</sub> adsorption isotherms (lines) with experimental data at 77 K. Experimental data is from ref 1 (squares), ref 14 (triangles), ref 15 (diamonds), and ref 16 (dots). Blue solid line: calculated isotherm with preserved rotational degrees of freedom of adsorbed H<sub>2</sub>; green dashed line: calculated isotherm for adsorbed H<sub>2</sub> with five vibrational motions relative to the MOF-5 surface; red solid line is calculated D<sub>2</sub> adsorption isotherm (D<sub>2</sub> rotations preserved). (Bottom) Calculated adsorption of H<sub>2</sub> on different sites in MOF-5 at 77 K.

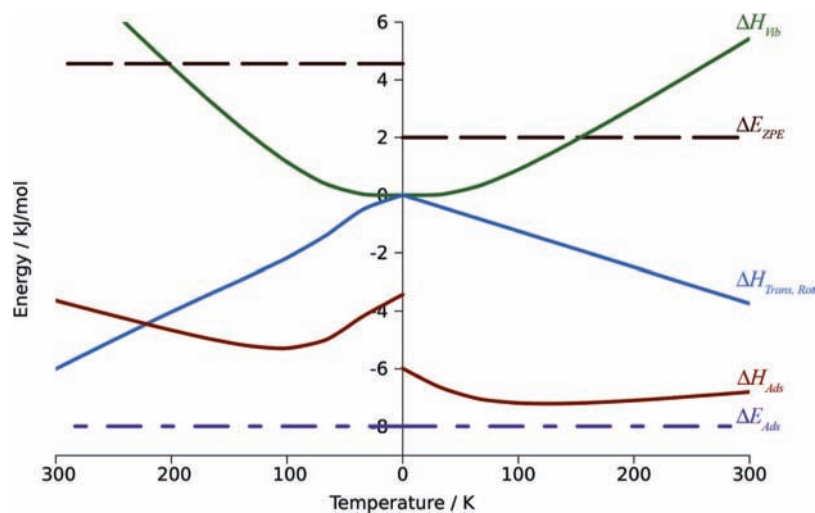


**Figure 5.** Different contributions to the adsorption enthalpy,  $\Delta H_{\text{Ads}}$ , assuming five vibrational modes of H<sub>2</sub> relative to the MOF-5 surface (left) and assuming that H<sub>2</sub> has retained its two rotational degrees of freedom and has three vibrational modes relative to the MOF-5 surface.  $\Delta H_{\text{Trans, Rot}}$  is the contribution of the translational and rotational degrees of freedom of H<sub>2</sub> to  $\Delta H_{\text{Ads}}$ .  $\Delta H_{\text{Vib}}$  is the sum of the vibrational contributions to  $\Delta H_{\text{Ads}}$ .  $\Delta E_{\text{Ads}}$  and  $\Delta E_{\text{ZPE}}$  are the energy and zero-point energy change upon adsorption, respectively.

differences, 70–80% correspond to the missing zero-point energies for the two vibrational modes that are substituted with rotations. FitzGerald et al.<sup>71</sup> report that the zero-point energy associated with the center-of-mass translational motion of H<sub>2</sub> in MOF-5 is of the order of 1.5 kJ/mol for three modes with a translational frequency of 84 cm<sup>-1</sup>. Our calculated values for three vibrational modes are between 1.1 and 2.0 kJ/mol.

Figure 5 shows how the different contributions to the adsorption enthalpy change with temperature taking H<sub>2</sub> on the α-site as example. The right part assumes that H<sub>2</sub> retains its two rotations on adsorption, whereas the left part assumes that rotations and translations are converted in 5 vibrations of H<sub>2</sub> relative to the MOF surface. There are no rotational or translational contribu-

tions from the models for MOF-5 and H<sub>2</sub>•••MOF-5 because they are part of the rigid solid. The translations (right) or translations and rotations (left) of H<sub>2</sub> in the gas phase make a negative contribution to the adsorption enthalpy that grows linearly with temperature and is responsible for the initial decrease of the adsorption enthalpy (Figures 5,  $\Delta H_{\text{Trans, Rot}}$ ). The vibrational contribution,  $\Delta H_{\text{Vib}}$ , is positive, and its nonlinear growth causes the increase of the adsorption enthalpy above 133 and 100 K (right and left part of Figure 5, respectively). It is dominated by the three (right) or five (left) vibrational modes of H<sub>2</sub> relative to the MOF-5 surface. The contribution of the H–H stretch mode to the adsorption enthalpy is constant below 400 K.

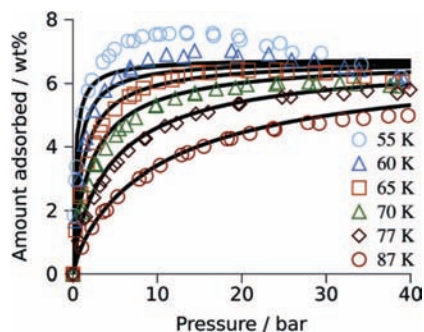


**Figure 6.** Calculated adsorption isotherms (solid black lines) for H<sub>2</sub> in MOF-5 at different temperatures. Data points are experimentally determined<sup>16</sup> amounts of H<sub>2</sub> adsorbed.

When H<sub>2</sub> retains its rotational degrees of freedom in the adsorbed state,  $\Delta H_{\text{Ads}}$  is more negative because  $\Delta E_{\text{ZPE}}$  is smaller, and it is less dependent on temperature (it goes from  $-6.0$  at 0 K to  $-7.2$  at 133 K, and then slowly decreases, reaching  $-6.8$  kJ/mol at 300 K).

**Multi-Langmuir Adsorption Isotherms.** Our calculated amount of adsorbed H<sub>2</sub> refers to excess adsorption which means that it is compared to the amount of H<sub>2</sub> in the gas phase at the same conditions. Our calculations treat H<sub>2</sub> in the gas phase as ideal gas and, thus, fail at low temperatures and very high pressures where intermolecular interactions can not be neglected.

In the present study the maximum adsorption capacity is limited to about 6.8 wt % which is the maximum amount of H<sub>2</sub> molecules that can adsorb on the adsorption sites considered. As can be seen from Figure 6, with exception to the above-mentioned conditions, our Multi-Langmuir approach reproduces experimental isotherms at different temperatures and over wide pressure range. Comparison with isotherms measured by Zhou et al.<sup>78</sup> give similar results. Furthermore, the present approach also works well for D<sub>2</sub>: Comparison with H<sub>2</sub> isotherms measured by FitzGerald et al.<sup>71</sup> shows an approximately 10% larger molar adsorption. This is well reproduced by our calculated isotherms which predict adsorbed amounts of 8.0 and 8.8 mmol/g, H<sub>2</sub> and D<sub>2</sub>, respectively, at 1 bar and 77 K, (Figure 4).

How sensitive are our adsorption results to a change of the input data for the individual sites? We have already mentioned that remaining uncertainties in the adsorption energies may change the amount H<sub>2</sub> adsorbed at 77 K and 40 bar from 6.0 to 5.6 wt %. Scaling all vibrational frequencies by 10%, much more than the expected uncertainty of the calculations reported in Table 3, will change the adsorbed amount from 6.0 to 6.2 wt % only.

The lower part of Figure 4 shows the population of different adsorption sites with increasing pressure at 77 K, which follows the order of increasing adsorption enthalpies. At low pressures the overall adsorption is determined by adsorption on  $\alpha$ -sites. The fact that the  $\alpha$ -sites are populated first is also supported by single-crystal neutron diffraction<sup>79</sup> and low-temperature neutron powder diffraction on different loading.<sup>2,79</sup>

Furthermore, the H<sub>2</sub> adsorption enthalpy calculated for the  $\alpha$ -site ( $-7.1$  kJ/mol) is well comparable with the initial heat of adsorption close to  $-7$  kJ/mol measured by Mulder et al.<sup>77</sup> and Dinca et al.<sup>80</sup> at very low hydrogen loadings. Moreover, Bordiga et al.<sup>7</sup> have observed sites in MOF-5 with adsorption enthalpies of  $-7.4$  kJ/mol. Upon adsorption on these sites the H–H frequency is shifted by  $-49$  cm<sup>-1</sup> which is in good correspondence with the  $-50$  cm<sup>-1</sup> calculated for the  $\alpha$ -site. Despite small differences in adsorption enthalpies (less than 0.5 kJ/mol), the coverage of the  $\gamma$ -site increases faster because of the larger number of  $\gamma$ -sites available. At a loading of four H<sub>2</sub> molecules per formula unit, there are three  $\alpha$ -sites and one  $\beta$ -site occupied with H<sub>2</sub> molecules. This is exactly what is witnessed in INS spectra.<sup>76</sup> Our calculations show that H<sub>2</sub> binding to  $\gamma$ -sites is possible only after H<sub>2</sub> adsorption on  $\alpha$ -sites because otherwise H<sub>2</sub> moves always from the  $\gamma$ -site to the more stable position on  $\alpha$ -site when there is no H<sub>2</sub> on the  $\alpha$ -site to prevent this (Figure 3). Previous DFT study of hydrogen adsorption in MOF-5 failed in this respect because neglecting dispersion interactions results in a different stability order of different adsorption sites.<sup>18</sup> On the whole, in accordance with numerous previous studies, we observe that H<sub>2</sub> binding to the inorganic part of the framework is preferred.

## Conclusions

Dispersion is the major contribution binding H<sub>2</sub> onto MOF-5, and the adsorption properties are determined by the local environment around the binding sites. Consequently, the use of DFT with an improper description of dispersion or the use of models that are too small with methods that include dispersion do not result in converged adsorption energies. Ab initio quantum chemistry (second-order Møller–Plesset perturbation theory) combined with molecular statistics makes an accurate description of the interactions between H<sub>2</sub> molecules and MOF-5 possible. We show that quantum effects must be taken into account when calculating adsorption enthalpies. With the method used we can reproduce measured adsorption isotherms if we assume that the adsorbed H<sub>2</sub> molecules have preserved their rotational degrees of freedom. The reference data presented here for the ideal structure allow discrimination between different isotherms measured for different MOF-5 samples and reliable prediction of isotherms for new MOF structures.

**Acknowledgment.** This work has been funded by the EU within the MOFCAT project under the NMP programme (Contract No. NMP4-CT-2006-033335). It has been also supported by German Research Foundation, priority program 1362.

**Supporting Information Available:** Comparison of CP-corrected MP2 and CCSD(T) H<sub>2</sub> adsorption energies for the  $\alpha$ -site. This material is available free of charge via the Internet at <http://pubs.acs.org>.

JA8099079

(78) Zhou, W.; Wu, H.; Hartman, M. R.; Yildirim, T. *J. Phys. Chem. C* **2007**, *111*, 16131–16137.

(79) Spencer, E. C.; Howard, J. A. K.; McIntyre, G. J.; Rowsell, J. L. C.; Yaghi, O. M. *Chem. Commun.* **2006**, 278–280.

(80) Dinca, M.; Han, W. S.; Liu, Y.; Dailly, A.; Brown, C. M.; Long, J. R. *Angew. Chem., Int. Ed.* **2007**, *46*, 1419–1422.